Available online at www.sciencedirect.com
SCIENCE DIRECT®
Catalysis Today 109 (2005) 178–184
CATALYSIS TODAY
www.elsevier.com/locate/cattod

Effect of hydrotreating conditions on Maya asphaltenes composition and structural parameters

F. Trejo [a,b], J. Ancheyta [b,*], G. Centeno [b], G. Marroquín [b,c]

[a] *Facultad de Química, UNAM, Ciudad Universitaria, México D.F. 04510, Mexico*
[b] *Instituto Mexicano del Petróleo, Eje Central Lázaro Cádenas 152,*
Col. San Bartolo Atepehuacan, México D.F. 07730, Mexico
[c] *Centro de Investigación en Ciencia Aplicada y Tecnología Avanzada del Instituto Politécnico Nacional,*
Legaria 694, México D.F. 11500, Mexico

Abstract

Hydrotreating of Maya crude was carried out in a pilot plant at different pressure, temperature and space-velocity, keeping constant the hydrogen-to-oil ratio. Pressure was varied in the range of 70–100 kg/cm^2, temperature between 380 and 420 °C, and space-velocity between 0.33 and 1.5 h^{-1}. Asphaltenes were precipitated from the feed and from hydrotreated products by using a batch reactor with *n*-heptane as solvent. Asphaltenes were characterized by elemental analysis, metals content, VPO aggregate molecular weight and NMR measurements. The effects of reaction conditions on asphaltene properties during hydrotreating are discussed in terms of changes in heteroatom contents and structural parameters.

Keywords: Asphaltenes; Hydrocracking; Structural parameters

1. Introduction

Crude oil is a complex molecular liquid in which micelles and molecular aggregates of different sizes and composition are found [1]. These micelles are formed by a heavy fraction called asphaltenes and are known to be dispersed by a fraction present in the crude oil called resin [2]. Petroleum asphaltenes are the heaviest aromatic component of crude oil.

It is well-known that heavy oil and residues can contain significant amounts of asphaltene that are responsible for the coke deposition that causes catalytic deactivation in the thermal and catalytic processing of petroleum residues. These processes can only be elucidated through an improved understanding of asphaltene chemistry [3].

The main problems caused by asphaltenes during catalytic hydroprocessing of heavy oils are: (1) they reduce the overall rate of the hydrodesulfurization (HDS) reaction, (2) they precipitate on the catalyst surface and block the pore mouth and (3) they act as coke precursors. However, the main impact from operational and economical points of view is that they may limit the maximum level of conversion due to sludge formation [4,5].

Vacuum residua are the most difficult feeds to convert catalytically because of their heavy molecular structures and impurity contents, such as sulfur, nitrogen and metals (mainly vanadium and nickel), concentrated in asphaltene fractions. Asphaltene content, asphaltene-to-resins ratio, the metal impurities level and the size of asphaltenes are critical properties for catalyst activity [6].

The molecular nature of petroleum asphaltenes has been the subject of numerous investigations. They appear to be very complex aromatic molecules surrounded and linked by aliphatic chains and heteroatoms. A great variety of analytical techniques have been employed to investigate asphaltene molecular structure. Particularly, ^{1}H and ^{13}C NMR provide reliable average molecular parameters such as aromatic carbon fraction (f_a), average number of carbon per alkyl side chains (n), average aromatic carbon substitution percent (A_s) and aromatic ring number (R_a) [7].

A wide range of average molecular weights, from 400 to 10,000 amu, has been reported using mass spectrometry, vapor pressure osmometry (VPO) and size-exclusion chromatogra-

---

[*] Corresponding author. Tel.: +52 55 9175 8443; fax: +52 55 9175 8429.
E-mail address: jancheyt@imp.mx (J. Ancheyta).

0920-5861/$ – see front matter © 2005 Elsevier B.V. All rights reserved.
doi:10.1016/j.cattod.2005.08.013

phy (SEC) [8]. The reasons given for the wide variety of asphaltene molecular weights are that they vary widely between different source crude oils and the value is highly dependent on both the method and measurement conditions. Methods such as VPO or GPC (gel permeation chromatography), in which solvents allow self-association, overestimate the asphaltene molecular weight [9]. Asphaltenes tend to associate both in their natural form and in solution [10]. Colloidal asphaltenic particles have been observed by small-angle scattering techniques in crude oil, in atmospheric and vacuum residues, as well as in various organic solvents [11].

Due to self-association propensity, molecular weight using vapor pressure osmometry corresponds to the molecular weight of asphaltene aggregates [12]. For this reason, measurements made by VPO will be considered in this work as aggregate molecular weight (AMW) [13].

X-ray diffraction (XRD) and small-angle X-ray scattering (SAXS) can also be used to obtain structural information from asphaltene aggregates [14]. XRD provides internal structural information and the crystallite parameters of the molecules associated in the aggregates. SAXS gives a topological view of the aggregate systems in which the X-rays are scattered by the electron density differences between the aggregate and the medium [15]. Since the asphaltenes are an extremely complex mixture of molecules, the use of a multidisciplinary approach through structure can be a useful means of investigating their chemical structure [4].

As was mentioned before, asphaltenes are coke precursors and deactivate the catalysts in heavy oils hydrotreating (HDT). According to Seki and Kumata [16], the HDS catalysts are mainly deactivated by coke. They reported that the molecular weight of both asphaltenes and resins measured by laser desorption mass spectrometry (LD–MS) decreases while HDT temperature is increased and asphaltenes tend to increase their aromaticity due to the shortening of alkyl side chains.

Merdrignac et al. [6] observed that the molecular weight of asphaltenes decreases as the severity of hydrotreating increases. Their observations were supported by size-exclusion chromatography. They explained the shift of the molecular weight distributions toward lower masses as a consequence of higher mass molecules that are preferentially converted to lighter ones due to the dealkylation of side alkyl chains during the hydrogenation process.

In a previous work [17], it was observed that asphaltenes precipitated from Maya crude and hydrotreated products exhibit different changes in composition during catalytic hydrotreating, depending on the severity of the reaction. At higher temperatures, nitrogen and metal content increases and sulfur content decreases, while asphaltene aromaticity, which was measured as aromaticity factor (f_a), increases.

In summary, literature reports indicate that hydrotreating can make the asphaltenes less soluble by removing their aliphatic chains. As the reaction temperature is increased, the H/C ratio of the asphaltenes is reduced. During severe hydrotreating it is observed that asphaltenes precipitate from the product. The asphaltene precipitation, which contributes to sludge formation, is undesirable when processing residual oil in the industry and the sulfur remaining in the product is predominantly found in the asphaltenic fraction [18].

Thus, the study of the changes of asphaltene properties during hydrotreating of heavy oil is an important concern nowadays. In the present paper, we precipitated asphaltenes from different hydrotreated products and the effects of reaction conditions on asphaltene properties are examined.

2. Experimental

2.1. Hydrotreating experiments

Maya crude oil was employed for all experiments and their main properties are shown in Table 1. Maya crude oil was hydrotreated in a pilot plant described in detail elsewhere [19]. The reactor temperature is maintained at the desired level by using a three-zone electric furnace, which provides an isothermal temperature along the active reactor section. Catalytic bed temperature is measured during the experiments by three thermocouples located in a thermowell mounted at the center of the reactor. The temperature profiles are measured by an axial thermocouple located inside the reactor. The reactor was checked for isothermal behavior and the greatest deviation from the desired temperature values was about 4–5 °C.

The catalyst employed for hydrotreating reactions was a commercial NiMo/Al_2O_3 sample (175 m^2/g specific surface area, 0.56 cm^3/g pore volume and 127 Å mean pore diameter). Different catalyst sizes were tested by crushing pellets and it was found that with 0.25 mm diameter particles, internal diffusion limitations can be neglected. One hundred milliliters of crushed catalyst was employed as catalytic bed. The catalyst was loaded to the reactor in the oxide form and it was sulfided in situ. Previously, the catalyst had been dried at 120 °C for 2 h using a hydrogen stream. After that, the catalyst was wetted with a straight-run gas oil stream, without stopping the hydrogen flow, at 150 °C for 2 h. Drying and wetting were both carried out at atmospheric pressure.

Table 1
Properties of Maya crude and of asphaltenes

	Maya crude	Asphaltenes
API gravity	20.9	
C (wt.%)	83.96	82.54
H (wt.%)	11.80	8.46
N (wt.%)	0.37	1.11
S (wt.%)	3.4	7.10
H/C atomic ratio	1.686	1.230
Insolubles in n-C_7 (wt.%)	12.4	–
V (wppm)	299	1509
Ni (wppm)	55	320
AMW	550	5190
R_a	–	62.0
A_s	–	38.9
n	–	6.80
f_a	–	0.52

Sulfiding was then carried out at the following conditions: pressure of 28 kg/cm^2, hydrogen-to-oil ratio of 2000 ft^3/bbl and LHSV of 2 h^{-1}. In the first stage, the temperature was set at 260 °C for 3 h. In the second stage, the temperature was increased up to 320 °C and maintained for 8 h. The catalyst was sulfided with a mixture of straight-run gas oil and dimethyl disulfide (1.0 wt.% sulfur). When sulfiding is completed, the feedstock is introduced and gas oil flow is stopped without stopping the hydrogen flow. The reactor temperature and other conditions, such as space-velocity and Maya crude flow, are adjusted to the reaction conditions.

The HDT experiments were conducted at the following operating conditions: pressure of 70, 85 and 100 kg/cm^2; H_2-to-oil ratio of 5000 ft^3/bbl; liquid hourly space-velocity of 0.33, 0.5, 0.75, 1.0, 1.25 and 1.5 h^{-1}; and reaction temperature of 380, 400 and 420 °C. Product samples were collected at 7–30 h intervals, after allowing an 8 h stabilization period under each set of conditions.

2.2. Precipitation of asphaltenes

Asphaltenes were precipitated by using *n*-heptane for solvent extraction in a Parr Batch Reactor Model 4842. The reactor is equipped with a stirring system, temperature control, pressure control and a vent. Hydrotreated products were put into the reactor and *n*-heptane was added. The solvent-to-hydrotreated products ratio was 5:1 (v/w).

A set of tests was carried out in order to find the precipitation conditions for having asphaltenes similar in amount and quality to those obtained with the standard and widely used ASTM-3279 Method. The best conditions were: pressure of 25 kg/cm^2, temperature of 60 °C and 750 rpm stirring rate. More details regarding these experiments were reported elsewhere [20].

Nitrogen was used as inert to pressurize the reactor. Stirring began until the temperature was adjusted to the desired value and it was continued for 30 min. After that, stirring was stopped and the sample was settled for 30 min. The reactor content was filtered using a vacuum system and a Whatman 934 AH filter paper with 1.5 μm pore size to retain the asphaltenes. Asphaltenes were washed using *n*-heptane until the filtered liquid was colorless. This assured maximum asphaltene purity.

2.3. Characterization of oils and asphaltenes

Nickel and vanadium contents of asphaltenes in Maya crude and in hydrotreated products were measured by atomic absorption using a SOLAAR AA Series Spectrometer analyzer. Carbon, hydrogen, nitrogen and sulfur contents in asphaltenes were determined by combustion in a Perkin-Elmer 2400 analyzer.

Aggregate molecular weight was measured by vapor pressure osmometry with a Corona Wescan 232A equipment and liquid state ^{1}H and ^{13}C NMR in a JEOL Eclipse 300 spectrometer operating at an ^{1}H resonance frequency of 300 MHz and a ^{13}C resonance frequency of 75 MHz, respectively. ^{1}H NMR spectra were obtained as deuterated chloroform ($CDCl_3$) solution with a flip angle of 75°, tube diameter of 5 mm and spectral width of 220 ppm, while ^{13}C NMR spectra were evaluated by applying an inverse-gated decoupling technique to suppress the NOE effect. Chromium acetylacetonate ($Cr(acac)_3$) was added to the final solution to ensure complete nuclear magnetic moment relaxation between pulses. In addition, tetramethylsilane (TMS) was employed as an internal reference. These conditions were necessary in order to have quantitative ^{13}C NMR signals. Operating conditions were as follows: a flip angle of 75°, a tube diameter of 5 mm, a $CDCl_3$ solvent and a spectral width of 220 ppm.

The measurements were performed for 30,000 scans in a gated proton decoupled mode. For ^{1}H NMR, the spectrum was divided into three regions (0.5–2 ppm: $\beta + \gamma$ hydrogen-to-aromatic ring, 2–4 ppm: α hydrogen-to-aromatic ring and 6–9 ppm: aromatic hydrogen) and the ^{13}C NMR spectrum was divided into only two different integration domains (10–60 ppm: aliphatic carbon and 110–160 ppm: aromatic carbon).

The main molecular parameters from NMR spectra are evaluated as follows [7]:

$$f_a = \frac{C_{ar}}{C_{ar} + C_{al}} \tag{1}$$

$$n = \frac{C_{al}}{C_{sub}} \tag{2}$$

$$A_s = 100 \times \left(\frac{\text{percent substituted aromatic carbon}}{\text{percent nonbridge aromatic carbon}} \right) \tag{3}$$

$$R_a = \frac{C_{ar} - C_p}{2} - 1 \tag{4}$$

where C_{ar} are the total aromatic carbons, C_{al} the total aliphatic carbons, C_{sub} the alkyl-substituted aromatic carbons and C_p the peripheral aromatic carbons ($C_p = C_{us} + C_{sub}$, where C_{us} are the unsubstituted aromatic carbons).

3. Results and discussion

3.1. HDT experiments

Table 1 presents some properties of the hydrotreating feed (Maya heavy crude). Properties of asphaltenes precipitated from this heavy oil are also shown in the table. It is evident that Maya crude is heavy in nature and hence a high percentage of heavy molecules is concentrated in its asphaltenes.

Nickel, vanadium and asphaltene contents were substantially reduced when Maya crude was hydrotreated. The reaction is highly severe when temperature and pressure are higher than 400 °C and 85 kg/cm^2, respectively and space-velocity lower than 1 h^{-1}. Temperature has a significant effect on asphaltene conversion favoring hydrocracking of asphaltenes at values higher than 400 °C.

Nickel and vanadium contents depend directly on how asphaltenes are converted. In Fig. 1, it is observed that the metal content (Ni + V) follows an approximately linear correlation

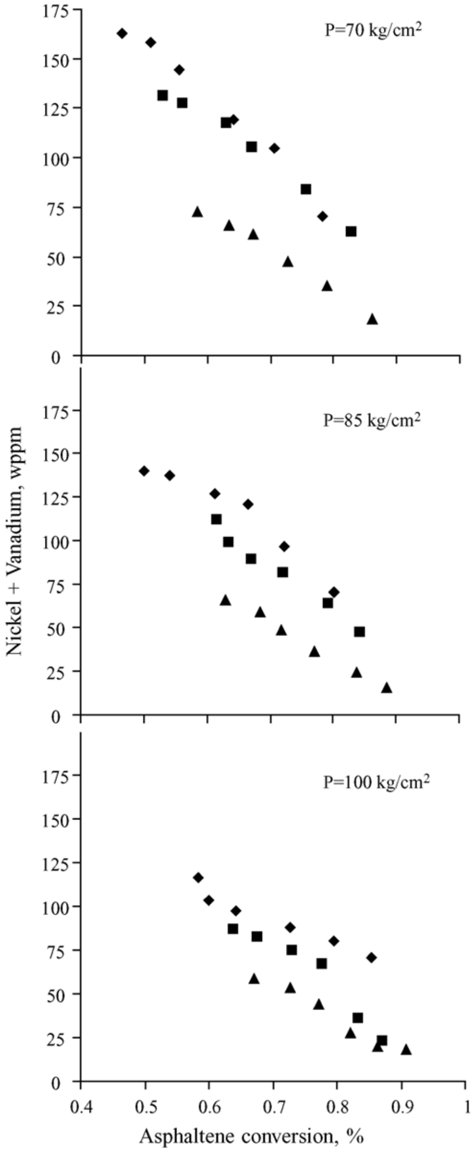

Fig. 1. Metals content as function of asphaltene conversion. (◆) 380 °C, (■) 400 °C, (▲) 420 °C.

with asphaltene conversion (HDAsp). This fact is more prominent at 70 and 85 kg/cm^2. Asphaltene removal is parallel to metal removal, a fact which suggests that metal porphyrin complexes in petroleum tend to concentrate and precipitate as part of the asphaltenic material [1].

3.2. Characterization of asphaltenes

The elemental analyses (C, H, N, S) of asphaltenes from selected hydrotreated products are shown in Table 2. As can be seen, carbon, hydrogen and sulfur contents progressively diminished as the severity of the reaction was increased. Nitrogen content remains almost constant since this heteroatom forms stable molecules when it is bounded in aromatic rings. Some authors [21] have reported that all nitrogen in asphaltenes is aromatic and that these compounds are located inside the asphaltene molecule.

Table 2
Elemental analysis of asphaltenes in n-C$_7$ from hydrotreated products

wt.%	70 kg/cm^2	85 kg/cm^2	100 kg/cm^2
400 °C and LHSV = 1			
C	84.00	83.97	83.82
H	7.02	6.98	6.96
N	1.50	1.47	1.44
S	3.52	3.46	3.41
H/C	1.003	0.997	0.996
wt.%	1.50 h^{-1}	1.00 h^{-1}	0.33 h^{-1}
100 kg/cm^2 and 400 °C			
C	84.10	83.82	83.35
H	7.01	6.96	6.86
N	1.47	1.44	1.34
S	3.45	3.41	3.32
H/C	1.000	0.996	0.988
wt.%	380 °C	400 °C	420 °C
100 kg/cm^2 and LHSV = 1			
C	83.85	83.82	83.71
H	6.98	6.96	6.94
N	1.44	1.44	1.43
S	3.47	3.41	3.32
H/C	0.999	0.996	0.995

The H/C atomic ratio of asphaltenes decreases as the temperature and pressure increase and LHSV is reduced, which indicates that more aromatic molecules are formed as a consequence of the breakage of side alkyl chains.

Table 3 presents Ni and V contents in asphaltenes from hydrotreated products. Both metal contents are increased as temperature and pressure are incremented. This behavior has been reported previously [17] and has been attributed to the reduction of alkyl side chains because of aliphatic carbon removal, whereas metals tend to remain unchanged and concentrate on the asphaltenes.

Table 3
Structural parameters and metals contents of asphaltenes in n-C$_7$ from hydrotreated products

	70 kg/cm^2	85 kg/cm^2	100 kg/cm^2
400 °C and LHSV = 1			
Ni (wppm)	311	325	385
V (wppm)	1601	1630	1682
R_a	28.32	27.86	25.90
A_s	33.89	34.29	32.70
	1.50 h^{-1}	1.00 h^{-1}	0.33 h^{-1}
100 kg/cm^2 and 400 °C			
Ni (wppm)	354	385	428
V (wppm)	1645	1682	1748
R_a	46.97	25.90	28.10
A_s	46.54	32.70	21.53
	380 °C	400 °C	420 °C
100 kg/cm^2 and LHSV = 1			
Ni (wppm)	311	385	433
V (wppm)	1637	1682	1698
R_a	40.18	25.90	31.35
A_s	36.61	32.70	26.95

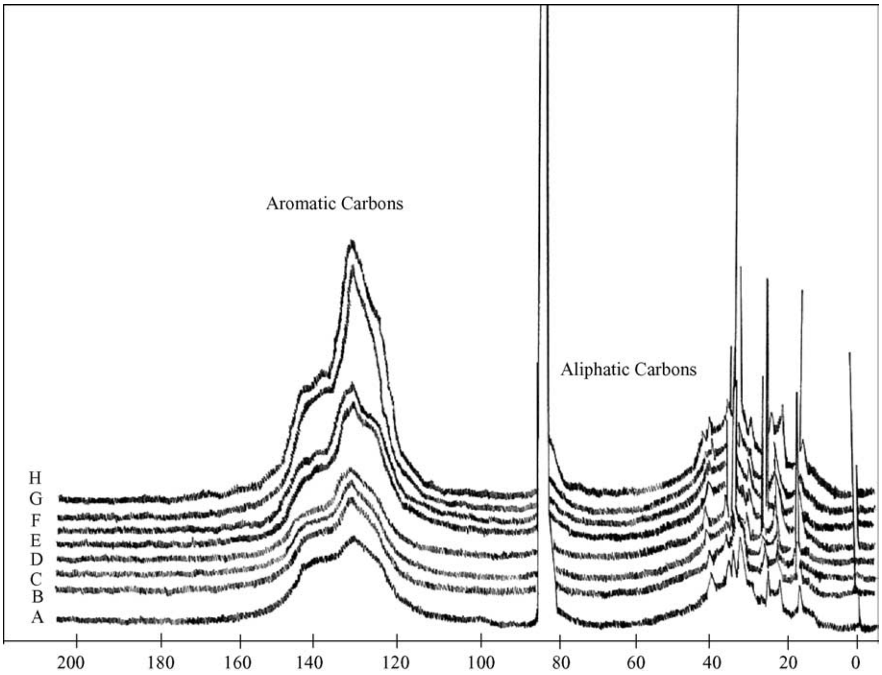

Fig. 2. NMR spectra of asphaltenes. (A) Maya crude asphaltenes; (B) 400 °C, 70 kg/cm^2, 1.0 LHSV; (C) 400 °C, 85 kg/cm^2, 1.0 LHSV; (D) 400 °C, 100 kg/cm^2, 1.5 LHSV; (E) 380 °C, 100 kg/cm^2, 1.0 LHSV; (F) 400 °C, 100 kg/cm^2, 1.0 LHSV; (G) 420 °C, 100 kg/cm^2, 1.0 LHSV; (H) 400 °C, 100 kg/cm^2, 0.33 LHSV.

Fig. 2 shows the ^{13}C NMR spectra of asphaltenes precipitated from Maya crude and from hydrotreated products obtained at different reaction conditions. The differences between aliphatic and aromatic peaks are noteworthy. Some structural parameters obtained by NMR are shown in Table 3. These structural parameters were calculated using Eqs. (1)–(4).

The aromatic rings number (R_a) generally tends to decrease when pressure and temperature are increased and space-velocity is reduced. The percent of substitution of aromatic rings (A_s) is also reduced as severity conditions are increased. These observations could lead to the discovery that poly-condensed rings are turned into other lighter fractions.

3.3. Effect of reaction conditions

3.3.1. Effect of the temperature

Fig. 3 shows the changes in asphaltenes structural parameters as a function of temperature when pressure and space-velocity are constant. When temperature increases, a shortening of the alkyl side chains occurs, and the average number of carbons gradually decreases. For this reason, there are less aliphatic carbons in asphaltenes, and aromatic carbons become predominant so that the H/C atomic ratio tends to decrease. This fact is supported by the increase in the aromaticity factor as a consequence of the high aromatic carbon content at higher temperatures.

The aggregate molecular weight was reduced as reaction temperature was increased, which indicates that the size of the asphaltene molecule is also decreased. The change in AMW is more drastic at the temperature value of 400 °C and higher, where more severe hydrocracking is carried out, and the

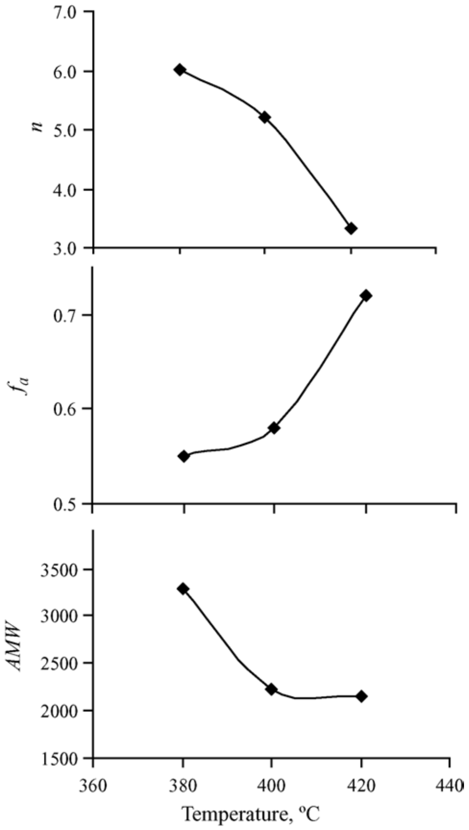

Fig. 3. Effect of temperature on the average number of carbons per alkyl side chain (n), aromaticity factor (f_a) and aggregate MW. $P = 100$ kg/cm^2, LHSV = 1.

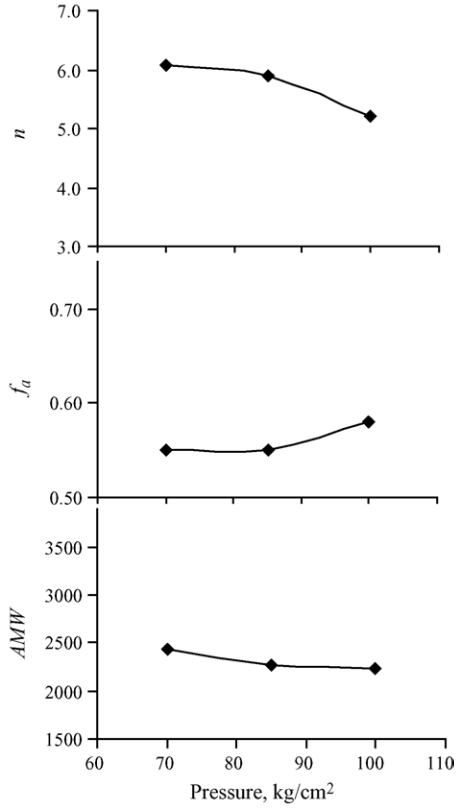

Fig. 4. Effect of pressure on the average number of carbons per alkyl side chain (n), aromaticity factor (f_a) and aggregate MW. $T = 400$ °C, LHSV = 1.

heteroatoms located at the external part of the asphaltene are released. Consequently, they are easily removed.

3.3.2. Effect of the pressure

Fig. 4 shows the effect of pressure on the properties of asphaltenes, keeping constant the space-velocity and the temperature. Similarly to the effect of temperature, alkyl side chains are reduced when pressure is increased. At high pressure, the aromaticity factor increases and the H/C atomic ratio decreases, which means that breakage of the aliphatic carbon in the side alkyl chains has occurred. There are not significant changes in the shortening of side alkyl chains at 70 and 85 kg/cm^2; however, at 100 kg/cm^2 the change is more prominent. The value of the aromaticity factor is also higher at 100 kg/cm^2.

Aggregate molecular weight is also diminished as pressure is increased. The most distinguishable change in this parameter is observed at 85 kg/cm^2. The combined effect of pressure and temperature shows that more severe hydrocracking is occurring when pressure is above 85 kg/cm^2 and temperature is higher than 400 °C.

3.3.3. Effect of the space-velocity

Fig. 5 shows how space-velocity affects some structural parameters of asphaltenes. When LHSV is low, the contact time (1/LHSV) between reactants and catalyst is high and conversion increases, which yields more hydrocracking selectivity. The number of carbons in alkyl side chains and aggregate molecular weight are reduced as space-velocity also decreases. The aromaticity factor tends to increase when space-velocity is lowered, and it is more evident at 0.33 h^{-1}.

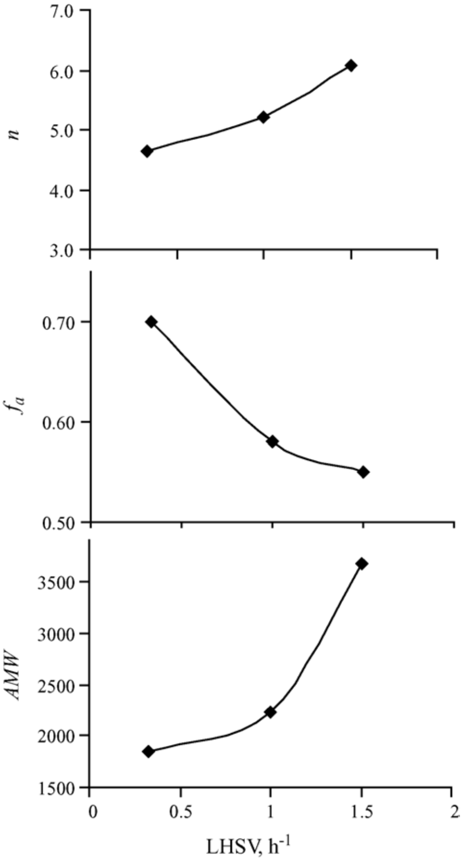

Fig. 5. Effect of space-velocity on the average number of carbons per alkyl side chain (n), aromaticity factor (f_a) and aggregate MW. $P = 100$ kg/cm^2, $T = 400$ °C.

As can be seen, AMW is drastically reduced when space-velocity is less than 1 h^{-1}. At 0.33 h^{-1}, it is almost half what it is when compared with aggregate molecular weight obtained at 1.5 h^{-1}. According to these results, the most severe hydrocracking occurs at 1 h^{-1} LHSV and below.

From all these observations, it can be established that hydrocracking of asphaltenes is more prominent at temperatures above 400 °C, pressure greater than 85 kg/cm^2 and space-velocity less than 1 h^{-1}.

Temperature presents the major influence on the shortening of the alkyl side chains. When it is increased from 400 to 420 °C, the average number of carbons per alkyl side chains changes from 5.22 to 3.34, which is even more remarkable compared with the effect produced by the increment of pressure and reduction of space-velocity.

Temperature produces the most important change in the aromaticity factor, which tends to increase drastically from 0.58 up to 0.72 when this variable is incremented from 400 to 420 °C. Space-velocity presents the same effect as temperature does; that is, the aromaticity factor is increased from 0.58 up to 0.70 when LHSV is reduced from 1.0 to 0.33 h^{-1}.

Space-velocity significantly influences the reduction of the AMW from 3666 to 2230 when LHSV is diminished from 1.5 to 1.0 h^{-1}. A similar effect is observed when temperature is increased from 380 up to 400 °C. In this range, the AMW reduces from 3284 to 2230.

In all cases, the effect of pressure is less significant than the effect of temperature and space-velocity on the shortening of alkyl side chains and on changes in the aromaticity factor and the reduction of AMW.

4. Conclusions

On the basis of these hydrocracking experiments and characterization results, it can be concluded that precipitated asphaltenes exhibit different changes in composition and in structural parameters depending on the severity of the reaction.

At the most severe experimental conditions, high temperature and pressure and low space-velocity, the asphaltene conversion percentages are close to 90%.

The relationship between hydrodeasphaltenization and metal removal showed an almost linear tendency, especially at pressures of 70 and 85 kg/cm^2.

Changes in structural parameters of asphaltenes supported the fact that metals concentrate in asphaltenes as the temperature is increased, since they are located inside the asphaltene structure and remain without change while the average number of carbons per alkyl side chain decreases.

Asphaltene aromaticity increased as temperature and pressure were also incremented and space-velocity was reduced. The H/C atomic ratio was slightly reduced and confirmed that asphaltenes became more aromatic at the most severe reaction conditions.

Acknowledgements

The authors thank the Instituto Mexicano del Petróleo for its financial support. F. Trejo also thanks the CONACyT and the UNAM for their financial support.

References

[1] J.G. Speight, The Chemistry and Technology of Petroleum, 2nd ed., Marcel Dekker, New York, 1991.
[2] J. Murgich, J. Rodríguez, J. Aray, Energy Fuels 10 (1996) 68–76.
[3] B. Avid, S. Sato, T. Takanohashi, I. Saito, Energy Fuels 18 (2004) 1792–1797.
[4] V. Calemma, P. Rausa, P. D'Antona, L. Montanari, Energy Fuels 12 (1998) 422–428.
[5] J. Ancheyta, G. Centeno, F. Trejo, G. Marroquín, J.A. García, E. Tenorio, A. Torres, Energy Fuels 16 (2002) 1121–1127.
[6] I. Merdrignac, C. Truchy, E. Robert, I. Guibard, S. Kressmann, Petrol. Sci. Techn. 22 (2004) 1003–1022.
[7] V. Calemma, P. Iwanski, M. Nali, R. Scotti, L. Montanari, Energy Fuels 9 (1995) 225–230.
[8] R. Tanaka, S. Sato, T. Takanohashi, J.E. Hunt, R.E. Winans, Energy Fuels 18 (2004) 1405–1413.
[9] J.T. Miller, R.B. Fisher, P. Thiyagarajan, R.E. Winans, J.E. Hunt, Energy Fuels 12 (1998) 1290–1298.
[10] C. Giavarini, D. Mastrofini, M. Scarsella, L. Barré, D. Espinat, Energy Fuels 14 (2000) 495–502.
[11] D.A. Storm, E.Y. Sheu, M. DeTar, Fuel 72 (1993) 977–981.
[12] E.Y. Sheu, Energy Fuels 16 (2002) 74–82.
[13] F. Trejo, G. Centeno, J. Ancheyta, Fuel 83 (2004) 2169–2175.
[14] J.W. Shirokoff, M.N. Siddiqui, M.F. Ali, Energy Fuels 11 (1997) 561–565.
[15] R. Tanaka, E. Sato, J.E. Hunt, R.E. Winans, S. Sato, T. Takanohashi, Energy Fuels 18 (2004) 1118–1125.
[16] H. Seki, F. Kumata, Energy Fuels 14 (2000) 980–985.
[17] J. Ancheyta, G. Centeno, F. Trejo, G. Marroquín, Energy Fuels 17 (2003) 1233–1238.
[18] J. Bartholdy, S.I. Andersen, Energy Fuels 14 (2000) 52–55.
[19] J. Ancheyta, S.K. Maity, G. Betancourt, G. Centeno, P. Rayo, M.T. Gómez, Appl. Catal. A 216 (2001) 195–208.
[20] G. Centeno, F. Trejo, J. Ancheyta, A. Carlos, Rev. Soc. Quím. Méx. 48 (2004) 186–195.
[21] S. Mitra-Kirtley, O.C. Mullins, J.V. Elp, S.J. George, J. Chen, S.P. Cramer, J. Am. Chem. Soc. 115 (1993) 252–258.